Second Virial Coefficients of Oligo- and Polystyrenes. Effects of Chain Ends

Yoshiyuki Einaga, Fumiaki Abe, and Hiromi Yamakawa*

Department of Polymer Chemistry, Kyoto University, Kyoto 606-01, Japan

Received July 27, 1993®

ABSTRACT: The second virial coefficient A_2 was determined from light scattering measurements for atactic polystyrene in cyclohexane at 34.5 °C (Θ) and in toluene at 15.0 °C down to the oligomer region, including the monomer, in order to clarify the effect of chain ends on A_2. The observed dependence of A_2 on weight-average molecular weight M_w may well be explained by the Yamakawa theory that takes into account both the effects of chain ends and chain stiffness. It is shown that the observed nonvanishing of A_2 at Θ arises from the former effect. The excess effective binary-cluster integrals β_1 and β_2 associated with the chain end beads are estimated to be 16 and 260 Å^3 in cyclohexane and 220 and 270 Å^3 in toluene, respectively, taking the repeat unit as a single bead. These values are of reasonable order of magnitude compared to those for small molecules. It is then striking to find that the effect of chain ends exists even at relatively large M_w ($\simeq 10^5$) in the good solvent toluene. For this system, however, the previous conclusion for the interpenetration function Ψ still remains valid, since the contribution $A_2^{(E)}$ of the effect of chain ends to A_2 is not very large in the ordinary range of M_w. As the cubed radius expansion factor α_S^3 (or M_w) is decreased, the (true) Ψ including no effect of $A_2^{(E)}$ in toluene first increases gradually, then passes through a maximum and a minimum, and finally increases steeply, deviating significantly upward from the two-parameter theory values but being consistent with the Yamakawa theory. This is due to the effect of chain stiffness. As α_S^3 (or M_w) is further decreased, the contribution of $A_2^{(E)}$ to A_2 or to the apparent interpenetration function Ψ_{ap} as usually defined from the whole A_2 including $A_2^{(E)}$ becomes progressively large. It is shown that the rapid increase of Ψ_{ap} there with decreasing M_w arises mainly from the effect of chain ends but not from that of chain stiffness, in contrast to the prevailing notion.

Introduction

In this series of experimental work on the excluded-volume effects in dilute solutions of oligomers and polymers,[1-3] we have shown that a *quasi*-two-parameter scheme is valid for the (gyration–)radius and viscosity–radius expansion factors α_S and α_η; i.e., both α_S and α_η may be expressed as functions only of the scaled excluded-volume parameter $\tilde{z}$ defined in the Yamakawa–Stockmayer–Shimada (YSS) theory[4-6] that takes into account the effects of excluded volume and chain stiffness. In contrast to these single-chain problems, the situation is rather involved for the second virial coefficient A_2, i.e., a two-chain problem. The recent theoretical analysis of A_2 by Yamakawa[7] has revealed that even for such large molecular weight M that the ratio of the unperturbed mean-square radius of gyration $\langle S^2\rangle_0$ to M already reaches its coil limiting value independent of M, the chain stiffness has a significant effect on the interpenetration function Ψ appearing in A_2, so that Ψ is not a universal function of α_S but its change with α_S depends separately on M and on the excluded-volume strength. The previous experimental results[8] for atactic polystyrene (a-PS) in various solvents have definitely confirmed the theoretical prediction in all aspects, indicating that neither the two-parameter scheme[9] nor even the quasi-two-parameter scheme is in general not valid for Ψ.

The Yamakawa theory[7] also predicts that the effect of chain ends on A_2 becomes appreciable for relatively small M. It gives a possible explanation of the nonvanishing of A_2 for small M at the Θ temperature (the temperature at which it vanishes for large M) as observed for a-PS in cyclohexane by light scattering (LS)[10] and small-angle X-ray scattering (SAXS)[11] and for atactic poly(methyl methacrylate) (a-PMMA) in acetonitrile by SAXS.[12] The theory may also well describe the observed dependence of A_2 on M for a-PS and a-PMMA with small M in good solvents[13,14] such that A_2 reaches a negative value after passing through a maximum as M is decreased. It has been further suggested[15] that the M independence of A_2 below Θ found for a-PS[16] may be explained by taking into account the effect of chain ends on A_2. However, the existent data for A_2 for oligomers are not so ample and accurate as to be subjected to quantitative analysis. Further, the terminal groups of the samples used have not been specified in some cases. Thus, in this study we determine A_2 of a-PS oligomers in cyclohexane at 34.5 °C (Θ) and in toluene at 15.0 °C from LS measurements by using well-characterized samples, and evaluate the contribution of the effect of chain ends to A_2. The solvent systems are the same as used in the previous studies of α_S,[1] α_η,[2] and A_2 (or Ψ).[8]

Attempts have sometimes been made to explain the observed nonvanishing of A_2 for small M at Θ in terms of the ternary-cluster integral or interaction. However, in the present work we make an analysis of experimental data for A_2 in Θ and good solvents only on the basis of the Yamakawa theory[7] that has been developed in the binary-cluster approximation. The reason for this is that none of the existent theories with consideration of the ternary-cluster integral can give a consistent explanation of A_2 at Θ and the M independence of Θ in its ordinary range,[17] and more importantly that the ternary-cluster terms may be regarded as negligibly small compared to the binary-cluster ones even for ordinary flexible polymers like a-PS as far as α_S and A_2 are concerned.[15]

Experimental Section

Materials. All the samples used in this work, except for the monomer (OS1), are the same as those used in the previous studies of the mean-square optical anisotropy $\langle\Gamma^2\rangle$,[18] the intrinsic viscosities $[\eta]_\Theta$[19] and $[\eta]$ ($=[\eta]_\Theta\alpha_\eta^3$),[2,3] the mean-square radii of gyration $\langle S^2\rangle_0$[11] and $\langle S^2\rangle$ ($=\langle S^2\rangle_0\alpha_S^2$),[1] the translational diffusion

* Abstract published in *Advance ACS Abstracts*, October 15, 1993.

0024-9297/93/2226-6243$04.00/0

Table I. Values of M_w, x_w, and M_w/M_n for Atactic Oligo- and Polystyrenes

sample	M_w	x_w	M_w/M_n
OS1	1.62×10^2	1	1.00
OS2[a]	2.66×10^2	2	1.00
OS3	3.70×10^2	3	1.00
OS5	5.78×10^2	5	1.00
OS6	6.80×10^2	5.98	1.00
OS8	9.04×10^2	8.13	1.01
A1000-a[b]	1.23×10^3	11.3	1.03
A2500-a[c]	2.27×10^3	21.3	1.05
A2500-b	3.48×10^3	32.9	1.07
A5000-3	5.38×10^3	51.2	1.03
F1-2	1.01×10^4	96.6	1.03
F2[b]	2.05×10^4	197	1.02

[a] M_w's of OS2 through OS8 had been determined from GPC.[18,19] [b] M_w's of A1000-a and F2 had been determined from LS in cyclohexane at 34.5 °C.[3,11] [c] M_w's of A2500-a through F1–2 had been determined from LS in methyl ethyl ketone at 25.0 °C.[18,19]

coefficient D,[20] and A_2 (or Ψ),[8] i.e., the fractions separated by preparative gel permeation chromatography (GPC) or fractional precipitation from the standard samples supplied by Tosoh Co., Ltd. They have a fixed stereochemical composition (the fraction of racemic diads $f_r = 0.59$) independent of molecular weight, and have an n-butyl group at one end of the chain (the initiating end) and hydrogen at the other (the terminating end). The monomer sample OS1 is n-hexylbenzene (or 1-phenylhexane) purchased from Aldrich Chemical Co., which has the same terminal groups as the other samples. It was purified by distillation under reduced pressure. The values of the weight-average molecular weight M_w, the weight-average degree of polymerization x_w, and the ratio of M_w to the number-average molecular weight M_n are listed in Table I. As seen from the values of M_w/M_n, all the samples are sufficiently narrow in molecular weight distribution, and in particular, the samples OS1 through OS5 are completely monodisperse.

The solvents cyclohexane and toluene were purified according to standard procedures prior to use.

Light Scattering. LS measurements were carried out to obtain A_2 (and also M_w) for all the a-PS samples in cyclohexane at 34.5 °C (Θ) and in toluene at 15.0 °C. A Fica 50 light scattering photometer was used for all the measurements with vertically polarized incident light of wavelength 436 nm. For a calibration of the apparatus, the intensity of light scattered from pure benzene was measured at 25.0 °C at a scattering angle of 90°, where the Rayleigh ratio $R_{Uu}(90°)$ of pure benzene was taken as 46.5×10^{-6} cm^{-1}. The depolarization ratio ρ_u of pure benzene at 25.0 °C was determined to be 0.41 ± 0.01 by the method of Rubingh and Yu.[21]

While the conventional method was used for solutions of the samples with $M_w > 10^3$, the new procedure previously presented[22] was applied to those of the oligomer samples with $M_w < 10^3$, since the concentration dependence of the density scattering R_d and the optical constant K has significant effects on the determination of A_2 (and also of M_w) in the latter. We give a short sketch of this procedure, for convenience. First, the isotropic Rayleigh ratio R_0 at vanishing scattering angle θ is obtained from the reduced total intensity R_{Uv}* of unpolarized scattered light for vertically polarized incident light, which includes the anisotropic contribution, by the use of the equation

$$R_0 = [1 - (7/6)\rho_u]R_{Uv}^* \quad (1)$$

Then, the excess Rayleigh ratio ΔR_0 arising from concentration fluctuations is determined by subtracting the density scattering R_d from R_0, i.e.,

$$\Delta R_0 = R_0 - R_d \quad (2)$$

It must be noted here that ρ_u and R_d are the quantities for a given solution of a finite concentration and that R_d cannot be directly determined but only calculated from the equation

$$R_d = (\kappa_T/\kappa_{T,0})[f(\tilde{n})/f(\tilde{n}_0)]R_{d,0} \quad (3)$$

with the observed value of the density scattering $R_{d,0}$ for the pure solvent. In eq 3, κ_T is the isothermal compressibility of the solution, $f(\tilde{n})$ is a function of the refractive index $\tilde{n}$ of the solution, and the subscript 0 refers to the value for the pure solvent. For $f(\tilde{n})$, it is appropriate to adopt the form

$$f(\tilde{n}) = (\tilde{n}^2 - 1)^2(\tilde{n}^2 + 2)^2 \quad (4)$$

which has been derived from the Lorentz–Lorenz equation for $\tilde{n}$ as a function of the density. Finally, ΔR_0 thus obtained is analyzed to determine A_2 from the equation

$$Kc/\Delta R_0 = M^{-1} + 2A_2'c + \ldots \quad (5)$$

where K is the optical constant, c is the mass concentration of the solute, and the light scattering second virial coefficient A_2' is related to A_2 by

$$A_2 = A_2' + RT\kappa_{T,0}/2M^2 \quad (6)$$

with R and T being the gas constant and the absolute temperature, respectively. Note that K in eq 5 includes $\tilde{n}$ and the refractive index increment $(\partial\tilde{n}/\partial c)_{T,p}$ at constant T and pressure p for a given solution of a finite concentration c.

In order to determine A_2 according to the above procedure, we measured R_{Uv}*, ρ_u, $\kappa_T/\kappa_{T,0}$, and $(\partial\tilde{n}/\partial c)_{T,p}$ for the oligomer solutions and also the first two quantities for the solvents. The values of $\tilde{n}$ at finite concentrations were calculated from the results for $(\partial\tilde{n}/\partial c)_{T,p}$ for each oligomer sample, as described below. The measurements of R_{Uv}* were carried out at angles θ ranging from 30 to 150°, and the mean of the values obtained at different θ was adopted as its value, since it must be independent of θ for oligomers. The values of ρ_u were obtained by the same method as employed in the calibration of the apparatus. We note that the correction for the anisotropic scattering was also applied to the solutions of the samples with $10^3 < M_w \leq 3.48 \times 10^3$ according to eq 1. The refractive index increment $(\partial\tilde{n}/\partial c)_{T,p}$ was determined as a function of c for each oligomer sample by the use of a Shimadzu differential refractometer. The ratio $\kappa_T/\kappa_{T,0}$ was measured with an apparatus constructed following the literature[23] (see below). The determination of A_2' from eq 5 was made by using the Berry square-root plot[24] and the Zimm plot.[25] We note that in the case of the conventional method we used the Berry plot as usual, and also the Bawn plot[26] for the cyclohexane solutions.

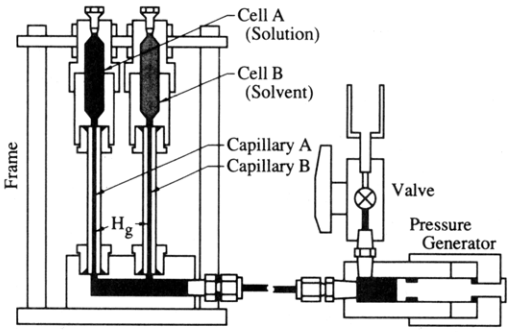

Figure 1. Schematic drawing of an apparatus for measurements of the isothermal compressibility.

Isothermal Compressibility. Figure 1 shows the schematic drawing of the apparatus used for the measurements of $\kappa_T/\kappa_{T,0}$. It consists of two cells A and B for the solution and solvent, respectively, which are connected to a mercury reservoir through capillary tubes A and B, joined with a pressure generator equipped with a valve for release of the applied pressure. The cells, capillary tubes, and mercury reservoir are tightly fixed on a metal frame, and the whole apparatus (except the pressure generator) is immersed in a thermostated water bath in order to keep the temperature of the solution and solvent constant. Both of the cells A and B have nearly the same volume of ca. 3.2 cm^3, and their inlets (or outlets) are small funnel-shaped openings which can be tightly closed with Teflon stoppers. The inner diameter of the capillaries is ca. 0.5 mm. Except for the glass capillaries, all the parts are made of stainless steel. The pressure generated by the pressure generator is applied via mercury to the solution and solvent which fill the cells A and B, respectively. It can be

raised to values larger than 100 atm. The change in the volume of the solution or solvent due to the applied pressure is detected as the change in the height of a meniscus of mercury in the capillary, which is measured to 0.01 mm with a traveling microscope.

Now the ratio $\kappa_T/\kappa_{T,0}$ is determined as follows. Let V_A and V_B be the volumes of the solution and solvent at pressure p, respectively, and let s_A (s_B) be the area of the cross section of the capillary A (B). Since the changes in V_A, V_B, κ_T, and $\kappa_{T,0}$ with p are negligibly small (each within ca. 1%) in its range of measurement, κ_T and $\kappa_{T,0}$ may be given by

$$\kappa_T = s_A \Delta h_A / V_A \Delta p$$
$$\kappa_{T,0} = s_B \Delta h_B / V_B \Delta p \quad (7)$$

where Δh_A (Δh_B) is the difference between the heights of meniscuses of mercury in the capillary A (B) at pressures $p \pm (1/2)\Delta p$, so that we have

$$\kappa_T/\kappa_{T,0} = C\Delta h_A/\Delta h_B \quad (8)$$

with C the apparatus constant given by

$$C = s_A V_B / s_B V_A \quad (9)$$

Thus, the ratio $\kappa_T/\kappa_{T,0}$ (at pressure p) may be obtained from eq 8 with the observed values of Δh_A and Δh_B if C is predetermined from eq 8 with the values of Δh_A and Δh_B measured for the same liquid, e.g., solvent filled in the cells A and B, in which case $\kappa_T/\kappa_{T,0}$ is unity. The value of the applied pressure p may then be determined if the difference Δp between p and the atmospheric pressure p^0 ($<p$) is known. Note that p^0 may be realized by opening the valve for pressure release and regarded as equal to 1 atm. This pressure difference Δp may be determined from

$$\Delta p = C'\Delta h_B/\kappa_{T,0} \quad (10)$$

with the observed value of Δh_B and the known value of $\kappa_{T,0}$, where Δh_B is the difference between the heights of meniscuses of mercury in the capillary B at p and p^0, and C' is another apparatus constant which is predetermined from

$$C' = s_B/V_B \quad (11)$$

with the known values of s_B and V_B.

From preliminary measurements using pure cyclohexane and benzene instead of the solution and solvent, we obtained the value $(1.23 \pm 0.03) \times 10^{-3}$ cm³/J for κ_T for pure cyclohexane at 34.5 °C by the use of the literature value $1.04_9 \times 10^{-3}$ cm³/J of $\kappa_{T,0}$ for pure benzene at 34.5 °C by Freyer et al.[27] and by Holder and Whalley.[28] This result for cyclohexane is in good agreement with the value $1.23_6 \times 10^{-3}$/J by the latter researchers.

In this work, we determined the ratio $\kappa_T/\kappa_{T,0}$ as a function of c and p for the oligomer samples of a-PS in cyclohexane at 34.5 °C (Θ) and in toluene at 15.0 °C. The pressure p was varied from 1 to ca. 50 atm. The solutions and solvent were maintained at a constant temperature within ±0.005 °C during the measurements.

Results

Isothermal Compressibility. Figure 2 shows plots of $\kappa_T/\kappa_{T,0}$ against p for the sample OS1 in cyclohexane at 34.5 °C (Θ) as an example at the indicated concentrations c, where the density of pure OS1 has been taken as the (highest) value of c in the bulk. It is seen that $\kappa_T/\kappa_{T,0}$ is independent of p within experimental error at any concentration in the range of p examined, as was assumed. Similar results were obtained for the other samples in cyclohexane at Θ and also in toluene at 15.0 °C. Thus, we adopted the mean of the results obtained at various pressures as the value of $\kappa_T/\kappa_{T,0}$ at p^0 (1 atm).

In Figure 3, values of $\kappa_T/\kappa_{T,0}$ are plotted against c for OS1 (unfilled circles), OS2 (top-half-filled circles), and OS3 (bottom-half-filled circles) in cyclohexane at Θ (upper part), and for OS5 (right-half-filled circles) and a Tosoh standard sample A-5000 (whose M_w and M_w/M_n are 5.57 × 10³ and 1.03, respectively, according to the supplier) (circles with bar) in toluene at 15.0 °C (lower part). The figure also includes the literature data for κ_T in the bulk for a mixture of styrene oligomers from the dimer to the pentamer (triangles) by Allen et al.[29] and for high-molecular-weight samples with $M_n = 5.1 \times 10^4$ and 8.2×10^4 (inverse triangles) by Höcker et al.[30] For these literature data, the values of $\kappa_T/\kappa_{T,0}$ have been calculated by the use of the values 1.23×10^{-3} and 8.69×10^{-4} cm³/J of $\kappa_{T,0}$ for pure cyclohexane at 34.5 °C (above) and for pure toluene at 15.0 °C by Freyer et al.,[27] respectively, and the densities have been taken as the values of c in the bulk (also for OS1 in cyclohexane at the highest c).

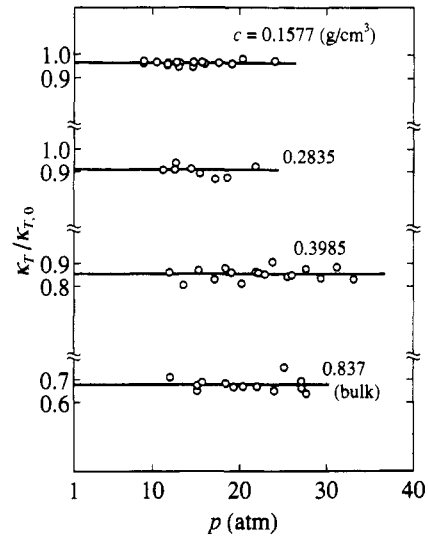

Figure 2. $\kappa_T/\kappa_{T,0}$ against p for the sample OS1 in cyclohexane at 34.5 °C at the indicated concentrations c. The value of c in the bulk represents the density of pure OS1.

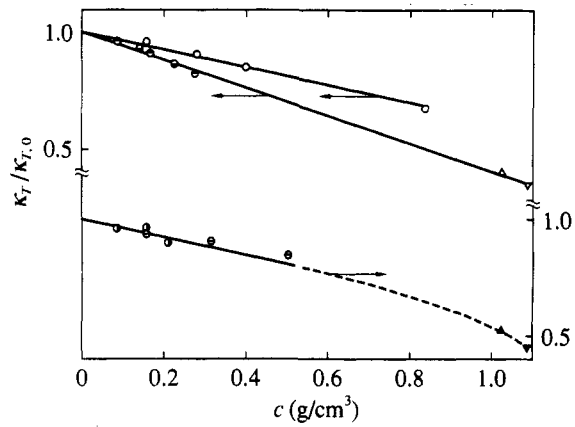

Figure 3. $\kappa_T/\kappa_{T,0}$ against c for a-PS: (○) OS1, (◒) OS2, (◒) OS3, (△) $x_w = 2$–5,[29] (▽) $M_n = 5.1 \times 10^4$ and 8.2×10^4,[30] in cyclohexane at 34.5 °C (upper part); (●) OS5, (⊖) A5000, (▲) $x_w = 2$–5,[29] (▼) $M_n = 5.1 \times 10^4$ and 8.2×10^4,[30] in toluene at 15.0 °C (lower part). The unfilled circle at the highest c and the triangles represent the values of the ratio with κ_T in the bulk (see the text).

As seen from Figure 3, $\kappa_T/\kappa_{T,0}$ for each sample in each solvent decreases with increasing c, following a straight line or a curve slightly convex upward. It is also seen that the data points form a single straight line for $x_w \geq 2$ for the cyclohexane solutions and a single composite curve for $x_w \geq 5$ for the toluene solutions, leading to the conclusion that the ratio $\kappa_T/\kappa_{T,0}$ in each solvent is independent of x_w in its range above. The present results may then be represented by the equation linear in c,

$$\kappa_T/\kappa_{T,0} \simeq 1 + kc \quad (12)$$

over the whole range of c for the cyclohexane solutions and for the $c \lesssim 0.5$ g/cm³ for the toluene solutions, as

Table II. Values of k_1 and k_2 in Equation 13 for Atactic Oligostyrenes in Cyclohexane at 34.5 °C (Θ) and in Toluene at 15.0 °C

	cyclohexane		toluene	
sample	k_1	k_2	k_1	k_2
OS1	0.0748	0.0095		
OS2	0.127	0		
OS3	0.153	−0.052		
OS5			0.0796	0
OS6			0.0848	0
OS8			0.0920	0

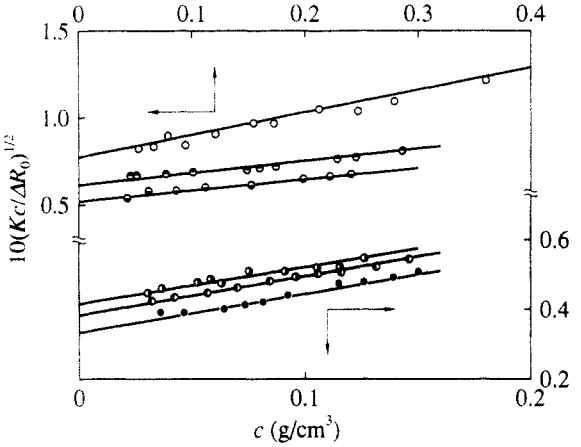

Figure 4. $(Kc/\Delta R_0)^{1/2}$ against c for the oligomer samples of a-PS: (○) OS1, (◒) OS2, (◒) OS3, in cyclohexane at 34.5 °C (Θ); (◑) OS5, (◐) OS6, (●) OS8, in toluene at 15.0 °C (see the text).

indicated by the solid straight lines in Figure 3. In eq 12, k is a constant independent of c and has been found to be −0.365 cm^3/g for OS1 in cyclohexane, −0.591 cm^3/g for $x_w \geq 2$ in cyclohexane, and −0.385 cm^3/g for $x_w \geq 5$ in toluene at the respective temperatures above.

Light Scattering from Oligostyrene Solutions. The results for $(\partial\tilde{n}/\partial c)_{T,p}$ at 436 nm determined to evaluate $\tilde{n}$ and K at finite concentrations c may be represented by the equation linear in c,

$$(\partial\tilde{n}/\partial c)_{T,p} = k_1 + k_2 c \qquad (13)$$

for $c < 0.40$ g/cm^3 in cyclohexane at 34.5 °C and for $c < 0.15$ g/cm^3 in toluene at 15.0 °C. In eq 13, k_1 and k_2 are constants independent of c, and their values are listed in Table II for each sample. The values of $\tilde{n}$ at c may be obtained from eq 13 by integration over c with $\tilde{n}_0 = 1.428$ for pure cyclohexane at 34.5 °C and $\tilde{n}_0 = 1.521$ for pure toluene at 15.0 °C. Thus, the values of ΔR_0 have been obtained from eq 2 with those of R_d calculated from eq 3 with eqs 4, 12, and 13.

Figure 4 shows the Berry square-root plots of ΔR_0 against c for OS1 (unfilled circles), OS2 (top-half-filled circles), and OS3 (bottom-half-filled circles) in cyclohexane at Θ, and for OS5 (right-half-filled circles), OS6 (left-half-filled circles), and OS8 (filled circles) in toluene at 15.0 °C, where the values of K containing $\tilde{n}$ and $(\partial\tilde{n}/\partial c)_{T,p}$ at finite concentrations c have been used. (We could not obtain the data for the samples with $x_w < 5$ in toluene, since the values of $(\partial\tilde{n}/\partial c)_{T,p}$ for their solutions were too small to determine ΔR_0 with sufficient accuracy.) In the figure, each straight line is a best fit to the data points such that its intercept gives the known value of M_w given in Table I and that the A_2' determined from its slope coincides with that from the Zimm plot. The reason for adopting this procedure is that it allows a more accurate determination of A_2' than the procedure of determining simultaneously A_2' and M_w as usual. (However, we note that the good fit of each straight line to the data points indicates

Table III. Results of LS Measurements on Atactic Oligo- and Polystyrenes in Cyclohexane at 34.5 °C (Θ) and in Toluene at 15.0 °C

	cyclohexane		toluene	
sample	$M_w \times 10^{-4}$	$A_2 \times 10^4$ (cm^3 mol/g^2)	$M_w \times 10^{-4}$	$A_2 \times 10^4$ (cm^3 mol/g^2)
OS1		100		
OS2		43		
OS3		33		
OS5				44
OS6				43
OS8				37
A1000-a	0.123	4.10	0.123	25
A2500-a	0.231	1.33	0.236	17
A2500-b			0.350	14.6
A5000-3[a]	0.544	0.41	0.537	12.2
F1-2	1.03	0.28		
F2	2.06	0.10	2.00	8.80
F4			3.94	6.45
F20			19.1	4.36
F40			35.7	3.72
F80			72.3	3.12
F128-2			129	2.81
F380			394	2.07

[a] M_w's and A_2's of A5000-3 through F380 in toluene at 15.0 °C have been reproduced from ref 8 except for F4, the values for which were not reported there, although already determined.

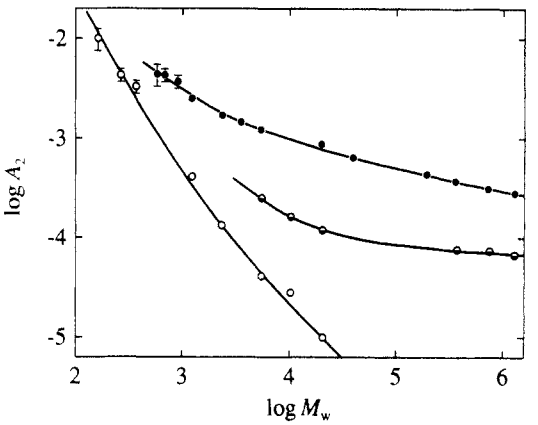

Figure 5. Double-logarithmic plots of A_2 against M_w for a-PS: (○) in cyclohexane at 34.5 °C (Θ), (●) in toluene at 15.0, (◒) in cyclohexane at 50.0 °C (previous data[8]). The vertical line segments indicate the error limit. The solid curves connect the data points smoothly.

that M_w and A_2' can be determined simultaneously with sufficient accuracy for such small M_w.)

The values of A_2' thus determined may be equated to those of A_2, since the second term on the right-hand side of eq 6 is negligibly small compared to A_2' in the present case. (This term is of order 10^{-5}–10^{-6} cm^3 mol/g^2, while A_2' is of order 10^{-2}–10^{-3} cm^3 mol/g^2, as shown below.)

Second Virial Coefficient. The values of A_2 determined from the present LS measurements are summarized in Table III along with those of M_w. It also includes the results for A_2 and M_w obtained previously[8] for higher-molecular-weight samples in toluene at 15.0 °C. Figure 5 shows double-logarithmic plots of A_2 in cyclohexane at 34.5 °C (Θ) (unfilled circles) and in toluene at 15.0 °C (filled circles) against M_w. It also includes the data obtained previously[8] for the same a-PS samples in cyclohexane at 50.0 °C (bottom-half-filled circles), for reference. The solid curves connect the data points smoothly. The vertical line segments attached to the data points for $M_w < 10^3$ indicate the limit of experimental error in A_2 caused mainly by the experimental uncertainty in ρ_u. We note that, among various quantities required to evaluate A_2, ρ_u is most difficult to determine with great accuracy and its

error has a serious effect on the accurate evaluation of A_2.

It is seen that, for the cyclohexane solutions at Θ, A_2 is definitely positive in the range displayed and increases steeply with decreasing M_w. This behavior is in qualitative agreement with the results by Huber and Stockmayer[10] from LS measurements and our previous results[7,11] from SAXS mentioned in the Introduction. The present results lead to the conclusion that the value of M_w above which A_2 at Θ becomes negligibly small (smaller than 5×10^{-6} $cm^3 mol/g^2$) is ca. 5×10^4. The data points for A_2 in toluene at 15.0 °C and in cyclohexane at 50.0 °C follow the curves concave upward, as indicated. That is, in these solvents, A_2 increases with decreasing M_w, more steeply for smaller M_w. All these steep increases of A_2 may be regarded as arising from the effect of chain ends.

Discussion

Effects of Chain Ends on A_2. We analyze the data for A_2 in Table III by the use of the Yamakawa theory[7] that considers the effect of chain ends on the basis of the helical wormlike (HW) touched-bead model. It is such that $n + 1$ beads are arrayed with spacing a between them along the contour of total length $L = na$, where the $n - 1$ intermediate beads are identical and the two end ones are different from the intermediate and also from each other in species. Identical excluded-volume interactions are expressed in terms of the conventional binary-cluster integral β, while two kinds of *excess* effective binary-cluster integrals, β_1 and β_2, are necessary to express interactions between unlike beads, β_1 being associated with one end bead and β_2 with two end ones. The HW model itself[31,32] is defined in terms of the three basic model parameters: the constant differential-geometrical curvature κ_0 and torsion τ_0 of its characteristic helix and the static stiffness parameter λ^{-1}.

According to the theory,[7] A_2 in general may be written in the form

$$A_2 = A_2^{(HW)} + A_2^{(E)} \tag{14}$$

where $A_2^{(HW)}$ is the part of A_2 without the effect of chain ends, i.e., that part of A_2 which vanishes at Θ, and $A_2^{(E)}$ represents the contribution of the effect of chain ends to A_2. The first term $A_2^{(HW)}$ may be written as

$$A_2^{(HW)} = (N_A c_\infty^{3/2} L^2 B / 2M^2) h \tag{15}$$

where N_A is Avogadro's number, and c_∞ and B are given by

$$c_\infty = \frac{4 + (\lambda^{-1}\tau_0)^2}{4 + (\lambda^{-1}\kappa_0)^2 + (\lambda^{-1}\tau_0)^2} \tag{16}$$

and

$$B = \beta / a^2 c_\infty^{3/2} \tag{17}$$

The h function is given by

$$h(\hat{z}) = (1 + 7.74\hat{z} + 52.3\hat{z}^{27/10})^{-10/27} \tag{18}$$

with

$$\hat{z} = \tilde{\tilde{z}} / \alpha_S^3 \tag{19}$$

In eq 19, $\tilde{\tilde{z}}$ is the intermolecular scaled excluded-volume parameter defined by[15]

$$\tilde{\tilde{z}} = [Q(\lambda L)/2/865]z \tag{20}$$

where the conventional excluded-volume parameter z is now defined by

$$z = (3/2\pi)^{3/2} (\lambda B)(\lambda L)^{1/2} \tag{21}$$

and Q is a function only of λL for ordinary flexible polymers and given by eq 19 of ref 7 for $\lambda L \gtrsim 1$.

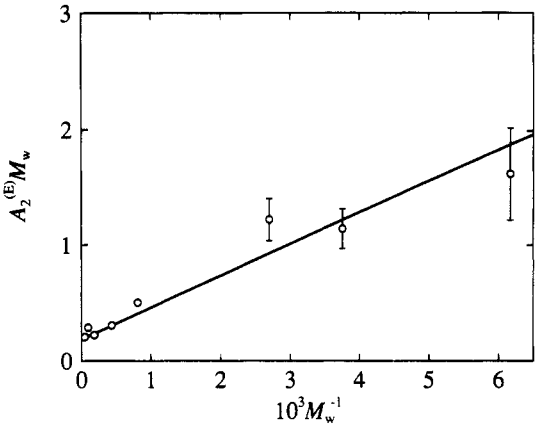

Figure 6. $A_2^{(E)}$ against M_w^{-1} for a-PS in cyclohexane at 34.5 °C (Θ). The vertical line segments indicate the error limit.

In the YSS theory,[4-6] α_S is assumed to be a function only of the intramolecular scaled excluded-volume parameter $\tilde{z}$ defined by

$$\tilde{z} = (3/4)K(\lambda L)z \tag{22}$$

where K is a function only of λL and given by eq 9 of ref 7, and the Domb–Barrett equation[33] for α_S is adopted with $\tilde{z}$ in place of z,

$$\alpha_S^2 = [1 + 10\tilde{z} + (70\pi/9 + 10/3)\tilde{z}^2 + 8\pi^{3/2}\tilde{z}^3]^{2/15} \times [0.933 + 0.067 \exp(-0.85\tilde{z} - 1.39\tilde{z}^2)] \tag{23}$$

Thus, note that h is a function of $\tilde{z}$ and $\tilde{\tilde{z}}$, and that eq 15 for $A_2^{(HW)}$ is valid for $\lambda L \gtrsim 1$, and we may put $h = 1$ approximately for $\lambda L \lesssim 1$. Recall that L is related to M by the equation

$$L = M/M_L \tag{24}$$

with M_L the shift factor defined as the molecular weight per unit contour length.

Now the second term $A_2^{(E)}$ in eq 14 may be written in the form

$$A_2^{(E)} = a_1 M^{-1} + a_2 M^{-2} \tag{25}$$

where

$$a_1 = 2N_A \beta_1 / M_0 \qquad a_2 = 2N_A \Delta\beta_2 \tag{26}$$

with M_0 the molecular weight of the bead and with

$$\Delta\beta_2 = \beta_2 - 2\beta_1 \tag{27}$$

The parameters β_1 and β_2 are explicitly defined in eqs 22 of ref 7.

It is seen from eq 25 that a_1 and a_2 may be determined from the intercept and slope, respectively, of the plot of $A_2^{(E)}M$ vs M^{-1}. In doing this, in the case of solutions in the Θ state, we may put $A_2 = A_2^{(E)}$, since then $A_2^{(HW)} = 0$ ($\beta = 0$). However, in the case of solutions in the non-Θ state, we must subtract $A_2^{(HW)}$ from A_2 to obtain $A_2^{(E)}$. We may then calculate $A_2^{(HW)}$ from eqs 15–24 with the values of the HW model parameters κ_0, τ_0, λ^{-1}, and M_L determined from, e.g., $\langle S^2 \rangle_0$ and the value of B (or λB) from α_S.

Figure 6 shows plots of $A_2^{(E)}M_w$ against M_w^{-1} for the data in cyclohexane at 34.5 °C (Θ), for which $A_2^{(HW)} = 0$ and $A_2^{(E)} = A_2$, as mentioned above. The vertical line segments indicate the error limit. Although the data points

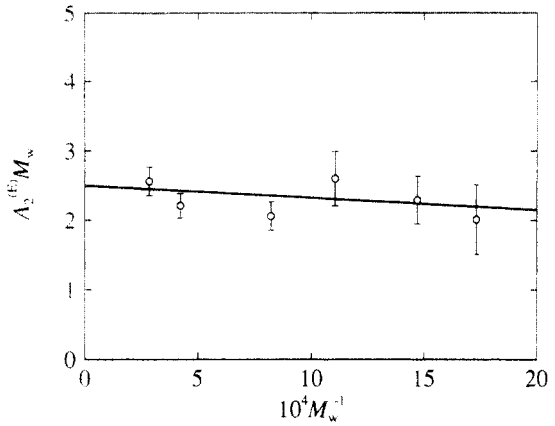

Figure 7. $A_2^{(E)}$ against M_w^{-1} for a-PS in toluene at 15.0 °C. The vertical line segments indicate the error limit.

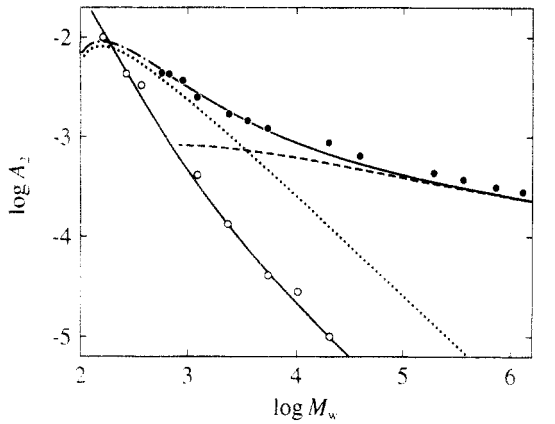

Figure 8. Comparison between the theoretical and observed values of A_2 as a function of M_w for a-PS in cyclohexane at 34.5 °C (Θ) and in toluene at 15.0 °C. The solid and chain curves represent the theoretical values of A_2, and the dashed and dotted curves those of $A_2^{(HW)}$ and $A_2^{(E)}$, respectively (see the text). The symbols have the same meaning as those in Figure 5.

somewhat scatter, they can be fitted by a straight line, confirming the validity of eq 25 which predicts that the nonvanishing of A_2 at Θ arises from the effect of chain ends. From the straight line, a_1 and a_2 are found to be 0.19 cm³/g and 270 cm³/mol, respectively. Then, β_1 and β_2 are determined to be 16 and 260 Å³, respectively, from eqs 26 and 27 with the above values of a_1 and a_2, taking the repeat unit as a single bead (M_0 = 104).

Next, we analyze the data in toluene at 15.0 °C in the range of M_w from 5.78×10^2 to 3.48×10^3, where the effect of chain ends is appreciable even in this good solvent. In this case, we must extract $A_2^{(E)}$ from the observed A_2 by calculating $A_2^{(HW)}$, as stated above. For this purpose, we have calculated $A_2^{(HW)}$ with the parameter values determined previously[1] from $\langle S^2\rangle_0$ and α_S, i.e., $\lambda^{-1}\kappa_0 = 3.0$, $\lambda^{-1}\tau_0 = 6.0$, $\lambda^{-1} = 20.6$ Å, $M_L = 35.8$ Å^{-1}, and $\lambda B = 0.26$, assuming that $h = 1$ for $L \lesssim 1$ (or $M_w \lesssim 737$). Figure 7shows plots of $A_2^{(E)}M_w$ against M_w^{-1} for the data of $A_2^{(E)}$ thus obtained. The data points again follow a straight line, which gives $a_1 = 2.5$ cm³/g and $a_2 = -200$ cm³/mol, and then $\beta_1 = 220$ Å³ and $\beta_2 = 270$ Å³ for the repeat unit. (Note that the β per repeat unit is found to be 33 Å³ from the above value of λB.)

The values of β_1 and β_2 determined above are of reasonable order of magnitude as the binary-cluster integrals associated with the end beads compared to those for small molecules.[34]

Molecular-Weight Dependence of A_2. Figure 8 shows double-logarithmic plots of A_2 against M_w for a-PS in cyclohexane at 34.5 °C (unfilled circles) and in toluene at 15.0 °C (filled circles). The solid curves represent the theoretical values calculated with the values of all the necessary parameters determined, as mentioned above. The chain curve represents those with $h = 1$ for the latter system, for which the theoretical contributions of $A_2^{(HW)}$ and $A_2^{(E)}$ are shown by the dashed and dotted curves, respectively. For the former system, for which $A_2 = A_2^{(E)}$, the agreement between theory and experiment is seen to be very good. For the latter system, the agreement is rather good; the theoretical values are somewhat (ca. 20%) smaller than the observed ones for $M_w > 10^4$. This may be regarded as arising from the fact that the theoretical h (or Ψ) function is underestimated except for very small and very large z (see also the next subsection). For the toluene solutions, $A_2^{(E)}$ is also seen to be so large as to remain significant even for $M_w > 10^5$, its contribution still amounting to several percent of A_2 at $M_w = 10^5$. It is 1 order of magnitude larger than that for the cyclohexane solutions for $M_w \gtrsim 10^3$.

It is interesting to see that the theory predicts a maximum of A_2 in toluene at 15.0 °C at $M_w \simeq 150$, although this has not been confirmed experimentally. In this connection, we note that Sotobayashi and Ueberreiter[13] have found long ago such behavior of A_2 experimentally for a-PS in naphthalene at 80.4 °C and obtained its negative value for the dimer, as mentioned in the Introduction. As shown in the Appendix, their results along with some other literature data[35-37] may be explained theoretically as well.

Interpenetration Function. We define the *apparent* interpenetration function Ψ_{ap} from the whole A_2 including the contribution $A_2^{(E)}$ of the effect of chain ends by the equation

$$\Psi_{ap} = A_2M^2/4\pi^{3/2}N_A\langle S^2\rangle^{3/2} \tag{28}$$

with $\langle S^2\rangle$ the perturbed mean-square radius of gyration. As is evident from its original physical meaning,[9] the true interpenetration function Ψ should now be redefined by

$$\Psi = A_2^{(HW)}M^2/4\pi^{3/2}N_A\langle S^2\rangle^{3/2} \tag{29}$$

In Table IV are listed the results for Ψ_{ap} and Ψ calculated for a-PS in toluene at 15.0 °C from eqs 28 and 29 with the values of A_2 in Table III and those of $A_2^{(HW)}$ obtained by subtraction of $A_2^{(E)}$ calculated with the above values of β_1 and β_2, respectively, along with those of α_S^3 and the reduced contour length λL. Here, we have used the previous results for $\langle S^2\rangle$ given in Tables II and III of ref 1 for the respective samples in the same solvent at the same temperature. (The value of $\langle S^2\rangle$ for the sample A1000-a has been obtained by interpolation from those for the oligomer samples given in Table II of ref 1.) In Figure 9,

Table IV. Values of Ψ_{ap}, Ψ, α_S^3, and λL for Atactic Oligo- and Polystyrenes in Toluene at 15.0 °C

sample	Ψ_{ap}	Ψ	α_S^3	λL
OS5	2.7	0.36	1	0.784
OS6	2.3	0.53	1	0.922
OS8	1.8	0.55	1	1.23
A1000-a	0.97	0.21	1	1.65
A2500-a	0.46	0.18	1.05	3.20
A2500-b	0.395	0.202	1.09	4.75
A5000-3	0.310	0.190	1.23	7.28
F2	0.325	0.279	1.30	27.1
F20	0.280	0.270	2.32	259
F40	0.264	0.257	2.89	484
F80	0.254	0.251	3.44	980
F128-2	0.249	0.249	4.31	1750
F380	0.252	0.252	5.59	5340

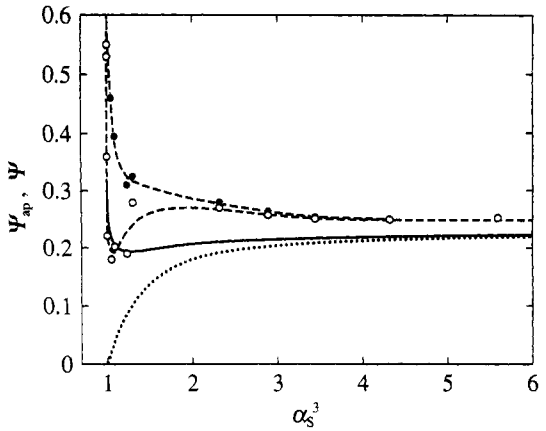

Figure 9. Ψ_{ap} and Ψ against α_S^3 for a-PS in toluene at 15.0 °C: (●) Ψ_{ap}, (○) Ψ. The dashed curves connect the respective data points smoothly. The solid curve represents the theoretical values of Ψ, and the dotted curve represents the two-parameter theory (coil limiting) values.

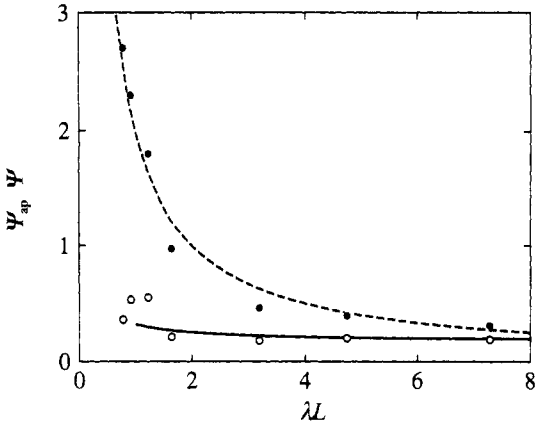

Figure 10. Ψ_{ap} and Ψ against λL for a-PS in toluene at 15.0 °C: (●) Ψ_{ap}, (○) Ψ. The dashed curve represents the empirical relation $\Psi_{ap} = 2/\lambda L$, and the solid curve represents the theoretical values of Ψ.

values of Ψ_{ap} (filled circles) and Ψ (unfilled circles) thus obtained are plotted against α_S^3. It does not include the values of Ψ_{ap} for the samples with $M_w \leq 1.23 \times 10^3$, which are too large to plot on this scale. The dashed curves connect the respective data points smoothly. The solid curve represents the theoretical values of Ψ calculated from[7,8]

$$\Psi = (6\langle S^2\rangle_0/c_\infty L)^{-3/2}(z/\alpha_S^3)h \qquad (30)$$

with eqs 16–23 and eq 1 of ref 7 with the values of the parameters given above (see also Figure 1 of ref 8). The dotted curve represents the two-parameter theory (coil limiting) values calculated from eq 30 with $\tilde{z} = \tilde{z} = z$.

From a comparison between Ψ_{ap} and Ψ, it is seen that the contribution of $A_2^{(E)}$ to Ψ_{ap} is negligibly small in the ordinary range of M_w, i.e., for $M_w \gtrsim 2 \times 10^5$ ($\alpha_S^3 \gtrsim 2.3$), the difference between Ψ_{ap} and Ψ amounting only to ca. 4% at $M_w \simeq 2.0 \times 10^5$. Thus, the previous conclusion[8] for Ψ for larger M_w in toluene at 15.0 °C still remains valid; i.e., Ψ increases monotonically with decreasing α_S^3 due to the effect of chain stiffness, deviating significantly upward from the two-parameter theory prediction. However, the contribution of $A_2^{(E)}$ is seen to become progressively large as M_w is decreased, leading to the split of Ψ from Ψ_{ap}. For $\alpha_S^3 \lesssim 2$, as α_S^3 is decreased, Ψ decreases, then passes through a minimum, and finally increases steeply. This is consistent with the theoretical prediction, although the theory underestimates Ψ for $1.3 \lesssim \alpha_S^3 \lesssim 6$. (Recall that the agreement between theory and experiment is good for larger α_S^3.[7]) On the other hand, Ψ_{ap} increases monotonically and steeply as α_S^3 is decreased to unity.

The steep increase of Ψ_{ap} at small M_w (or α_S^3 close to unity) has been previously explained as follows.[7,10] As M (or L) is decreased, the behavior of the chain becomes rodlike, so that $\langle S^2\rangle \propto M^2$ and $A_2 \propto M^0$ in eq 28, thereby leading to

$$\Psi_{ap} \propto M^{-1} \propto (\lambda L)^{-1} \text{ (long rods)} \qquad (31)$$

However, this explanation is not necessarily reasonable. The reason for this is that eq 31 is valid only for *long* rigid rods, while the actual chain molecules become *short* rigid rods as M is decreased. Indeed, as seen from Figures 5 and 8, A_2 is not independent of M for small M.

In Figure 10, values of Ψ_{ap} (filled circles) and Ψ (unfilled circles) are plotted against the reduced contour length λL for the samples with $M_w < 10^4$ in toluene at 15.0 °C. As seen from the figure, Ψ_{ap} increases steeply with decreasing λL, being in agreement with the results obtained by Huber and Stockmayer[10] for a-PS with $M_w > 10^3$ in toluene. This result seems apparently consistent with eq 31, since the data points may be fitted rather well by the dashed curve calculated from the empirical equation $\Psi_{ap} = 2/\lambda L$. However, it is clear that the sharp increase of Ψ_{ap} arises from the effect of chain ends, i.e., the contribution of $A_2^{(E)}$. Indeed, the increase of the true Ψ with decreasing M_w is gradual. Note that the data points are essentially equivalent to the theoretical values represented by the solid curve, as is natural from the above calculation of the former.

Concluding Remarks

In this work, we have determined A_2 for a-PS in the Θ and good solvents down to the oligomer region, including the monomer, from light scattering measurements, following the procedure previously[22] proposed for oligomer solutions. It has been found that the observed molecular weight dependence of A_2 may well be explained by the theory[7] that takes into account the effect of chain ends. The values obtained for the excess effective binary-cluster integrals β_1 and β_2 associated with the beads at the chain ends are of reasonable order of magnitude compared to those of the binary-cluster integrals for small molecules.[34] The present results show that the effect of chain ends on A_2, i.e., $A_2^{(E)}$, exists even at rather large M_w ($\simeq 10^5$) in the good solvent. However, since its contribution to A_2 becomes progressively small with increasing M_w, the previous conclusion[7,8] still remains valid for larger M_w; i.e., Ψ as a function of α_S^3 deviates significantly upward from the two-parameter theory prediction due to the effect of chain stiffness in the ordinary range of M_w. It has been found that the true Ψ including no effect of chain ends has a minimum at small M_w (α_S^3 close to unity) and increases steeply with further decreasing α_S^3, being also consistent with the theoretical prediction. On the other hand, it has been shown that the observed rapid increase of the apparent interpenetration function Ψ_{ap} defined as usual from the whole A_2 with decreasing M_w for small M_w arises mainly from the effect of chain ends but not from the effect of chain stiffness, in contrast to the prevailing notion.

In the present paper, we have not considered the contribution of the ternary-cluster integral to A_2 (and also α_S) from the start, following the recent analysis by Yamakawa.[15] It predicts that its contribution is negligibly small compared to that of the binary-cluster integral β. This is due to the fact that the probability of triple (or

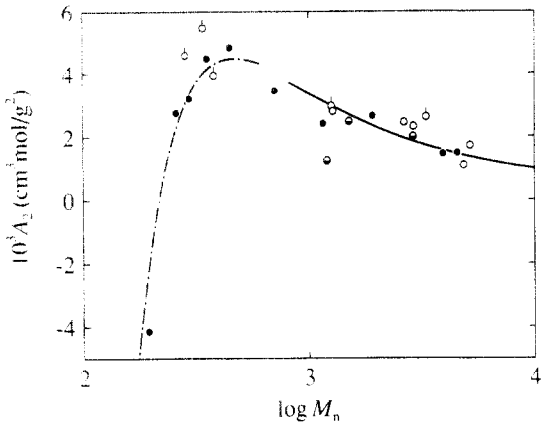

Figure 11. Comparison between the theoretical and observed values of A_2 as a function of M_n for a-PS: (●) in naphthalene at 80.4 °C,[13] (◒) for the samples with trichloro–triphenyl–methyl end groups in naphthalene at 80.4 °C,[35] (◔) in benzene at 5.49 °C.[36] (○) in benzene at 5.49 °C,[37] (solid and chain curves) theoretical values (see the text).

multiple) bead contact is much smaller than that of double contact because of the chain stiffness. The former probability must become smaller and smaller as the chain becomes short.

Finally, it is important to note that the effect of chain ends as considered by Yamakawa[15] exists not only in the case for which the chain has specific terminal groups, but also in the case for which the terminal groups are the monomer units. The reason for this is that even in the latter case the terminal groups are different from the intermediate repeat units and also the isolated monomer molecule itself in chemical structure. Thus, the effect must always be taken into account in the oligomer region, and also even in the ordinary range of M_w if relatively small.

In a forthcoming paper, we make a similar study of $A_2^{(E)}$, Ψ_{ap}, and Ψ for a-PMMA in various solvents, which is quite different from a-PS in chain stiffness and local chain conformation.

Acknowledgment. This research was supported in part by a Grant-in-Aid (02453100) from the Ministry of Education, Science, and Culture, Japan.

Appendix. Analysis of Literature Data

According to the procedure described in the text, we analyze the literature data obtained from cryoscopic experiments for a-PS oligomers in naphthalene at 80.4 °C[13,35] and in benzene at 5.49 °C.[36,37] In one of these experiments, the data were taken for the samples with trichloro–triphenyl–methyl end groups,[35] while in the other the chemical structures of the end groups are unknown. Further, we ignore the differences in the solvent and temperature, since the data in the two solvents coincide with each other within experimental error. In order to calculate $A_2^{(HW)}$, we assume that $h = 1$, and adopt the values of the HW model parameters and λB determined in our previous paper[3] for a-PS in benzene at 25.0 °C (the values determined from $\langle S^2 \rangle_0$ in *trans*-decalin at Θ and α_S in benzene at 25.0 °C), i.e., $\lambda^{-1}\kappa_0 = 3.0$, $\lambda^{-1}\tau_0 = 6.0$, $\lambda^{-1} = 19.4$ Å, $M_L = 35.8$ Å^{-1}, and $\lambda B = 0.33$.

The results obtained for β_1 and β_2 per repeat unit are 270 and −72 Å^3, respectively. Figure 11 shows plots of A_2 against log M_n for a-PS in naphthalene (filled and half-filled circles) and in benzene (unfilled circles with and without pip). The curves have the same meaning as in Figure 8. It is seen that there is good agreement between theory and experiment. In particular, the theory may explain the observation that A_2 exhibits a maximum at $M_n \simeq 450$ and becomes negative for the dimer.

References and Notes

(1) Abe, F.; Einaga, Y.; Yoshizaki, T.; Yamakawa, H. *Macromolecules* **1993**, *26*, 1884.
(2) Abe, F.; Einaga, Y.; Yamakawa, H. *Macromolecules* **1993**, *26*, 1891.
(3) Horita, K.; Abe, F.; Einaga, Y.; Yamakawa, H. *Macromolecules* **1993**, *26*, 5067.
(4) Yamakawa, H.; Stockmayer, W. H. *J. Chem. Phys.* **1972**, *57*, 2843.
(5) Yamakawa, H.; Shimada, J. *J. Chem. Phys.* **1985**, *83*, 2607.
(6) Shimada, J.; Yamakawa, H. *J. Chem. Phys.* **1986**, *85*, 591.
(7) Yamakawa, H. *Macromolecules* **1992**, *25*, 1912.
(8) Yamakawa, H.; Abe, F.; Einaga, Y. *Macromolecules* **1993**, *26*, 1898.
(9) Yamakawa, H. *Modern Theory of Polymer Solutions*; Harper & Row: New York, 1971.
(10) Huber, K.; Stockmayer, W. H. *Macromolecules* **1987**, *20*, 1400.
(11) Konishi, T.; Yoshizaki, T.; Saito, T.; Einaga, Y.; Yamakawa, H. *Macromolecules* **1990**, *23*, 290.
(12) Tamai, Y.; Konishi, T.; Einaga, Y.; Fujii, M.; Yamakawa, H. *Macromolecules* **1990**, *23*, 4067.
(13) Sotobayashi, H.; Ueberreiter, K. *Z. Elektrochem.* **1963**, *67*, 178.
(14) Springer, J.; Ueberreiter, K.; Moeller, E. *Z. Elektrochem.* **1965**, *69*, 494.
(15) Yamakawa, H. *Macromolecules* **1993**, *26*, 5061.
(16) Tong, Z.; Ohashi, S.; Einaga, Y.; Fujita, H. *Polym. J.* **1983**, *15*, 835.
(17) Nakamura, Y.; Norisuye, T.; Teramoto, A. *Macromolecules* **1991**, *22*, 4904.
(18) Konishi, T.; Yoshizaki, T.; Shimada, J.; Yamakawa, H. *Macromolecules* **1989**, *22*, 1921.
(19) Einaga, Y.; Koyama, H.; Konishi, T.; Yamakawa, H. *Macromolecules* **1989**, *22*, 3419.
(20) Yamada, T.; Yoshizaki, T.; Yamakawa, H. *Macromolecules* **1992**, *25*, 377.
(21) Rubingh, D. N.; Yu, H. *Macromolecules* **1976**, *9*, 681.
(22) Einaga, Y.; Abe, F.; Yamakawa, H. *J. Phys. Chem.* **1992**, *96*, 3948.
(23) Kim, Y. B.; Ogino, K. *Phys. Lett.* **1977**, *61A*, 40.
(24) Berry, G. C. *J. Chem. Phys.* **1966**, *44*, 4550.
(25) Zimm, B. H. *J. Chem. Phys.* **1948**, *16*, 1093.
(26) Norisuye, T.; Fujita, H. *ChemTracts: Macromol. Chem.* **1991**, *2*, 293.
(27) Freyer, E. B.; Hubberd, J. C.; Andrews, D. H. *J. Am. Chem. Soc.* **1929**, *51*, 759.
(28) Holder, G. A.; Whalley, E. *Trans. Faraday Soc.* **1962**, 58, 2095.
(29) Allen, G.; Gee, G.; Mangaraj, D.; Sims, D.; Wilson, G. J. *Polymer* **1960**, *1*, 467.
(30) Höcker, H.; Blake, G. J.; Flory, P. J. *Trans. Faraday Soc.* **1971**, *67*, 2251.
(31) Yamakawa, H. *Annu. Rev. Phys. Chem.* **1984**, *35*, 23.
(32) Yamakawa, H. In *Molecular Conformation and Dynamics of Macromolecules in Condensed Systems*; Nagasawa, M., Ed.; Elsevier: Amsterdam, 1988; p 21.
(33) Domb, C.; Barrett, A. J. *Polymer* **1976**, *17*, 179.
(34) Yamakawa, H.; Fujii, M. *J. Chem. Phys.* **1973**, *58*, 1523.
(35) Ueberreiter, K.; Rohde-Liebenau, U. *Makromol. Chem.* **1961**, *49*, 164. For the A_2 data, see: Sotobayashi, H.; Springer, J. *Adv. Polym. Sci.* **1969**, *6*, 473.
(36) Kemp, A. R.; Peters, H. *Ind. Eng. Chem.* **1942**, *34*, 1097.
(37) Schulz, G. V.; Marzolph, H. *Z. Elektrochem.* **1954**, *58*, 211.